

pubs.acs.org/JACS Communication

Molecular Photothermal Conversion Catalyst Promotes Photocontrolled Atom Transfer Radical Polymerization

Cristina Preston-Herrera, Sajjad Dadashi-Silab, Daniel G. Oblinsky, Gregory D. Scholes, and Erin E. Stache*



Cite This: J. Am. Chem. Soc. 2024, 146, 8852-8857



ACCESS I

Metrics & More

Article Recommendations

SI Supporting Information

ABSTRACT: Photothermal conversion is a growing research area that promotes thermal transformations with visible light irradiation. However, few examples of dual photothermal conversion and catalysis limit the power of this phenomenon. Here, we take inspiration from nature's ability to use porphyrinic compounds for nonradiative relaxation to convert light into heat to facilitate thermal polymerization catalysis. We identify the photothermal conversion catalytic activity of a vitamin B₁₂ derivative, heptamethyl ester cobyrinate (HME-Cob), to perform atom transfer radical polymerization (ATRP) under irradiation. Rapid polymerization are obtained under photothermal activation while maintaining good control over polymerization with the aid of a photoinitiator to enable light-induced catalyst regeneration. The catalyst exhibits exquisite temporal control in photocontrolled thermal polymerization. Ultimately, the activation of this complex is accessed across a broad range of wavelengths, including near-IR light, with excellent temporal control. This work showcases the potential of developing photothermal conversion catalysts.

Photothermal conversion is a powerful tool for conducting thermal transformations using visible light irradiation. Photothermal conversion agents can generate localized heat by converting light to thermal energy, thereby enabling highly selective reactions with spatial and temporal control.² While heat alone can overcome high activation barriers, combination with other forms of catalysis can facilitate more sophisticated reactions. Much effort has been made toward developing colloidal or macroscopic photothermal agents, such as precious metal-based nanoparticles, semiconductors, or metal-organic frameworks, to promote energy-intensive reactions under mild photochemical conditions.^{3–8} However, this strategy relies on localized surface plasmonic resonance, a highly wavelengthspecific phenomenon (Figure 1A).⁴ Additionally, competing energy and electron transfer pathways can complicate the reaction development.

Alternatively, inexpensive, abundant, carbon-based photothermal agents generate localized heat on the surface of the material via photoexcitation of electrons that move around the carbon-based lattice (Figure 1B). Through heat generation, these materials can mediate high activation barrier reactions using broad wavelength irradiation. 10-15 However, the reactivity of carbon-based nanomaterials is primarily limited to heat generation via photothermal conversion without any inherent catalytic reactivity. Chromophores represent a third class of photothermal conversion agents. The nonradiative decay pathway via molecular vibrations has been observed in molecular dyes (Figure 1C).¹⁶ An example of this mechanism can be seen in nature where plants can dissipate the excess photonic energy as heat using photothermal conversion enabled by chlorophyll. 17,18 However, there is limited research into identifying and developing photothermal conversion catalysts that promote photocontrolled thermal reactions.

Porphyrinic compounds, such as chlorophyll, heme, aluminum, and zinc porphyrin, have been reported to show photothermal conversion effects upon irradiation with visible light. These and related metallomacrocycles provide a modular platform for developing molecular photothermal conversion agents with catalytic activity to unlock new reactivities in thermal transformations controlled by light. Although structurally resembling porphyrins, corrin complexes found in vitamin B_{12} derivatives are underexplored as photothermal conversion catalysts. The corrin macrocycle possesses a lower degree of conjugation compared with the porphyrins, 24 which allows molecular flexibility and non-radiative relaxation pathways to be favored when photoexcited. The porphyrins of the property of the pr

We hypothesized that vitamin B₁₂ complexes would serve as molecular photothermal conversion agents akin to other naturally occurring porphyrinic compounds. ¹⁹ Our group recently developed a strategy to use heptamethyl ester cobyrinate (HME-Cob), a hydrophobic vitamin B₁₂ derivative, as a cobalt catalyst for atom transfer radical polymerization (ATRP) under thermal conditions. ²⁶ We envisioned that upon irradiation, HME-Cob could be used as a molecular photothermal conversion catalyst to mediate ATRP with temporal control. We posit that under light irradiation, the HME-Cob complex undergoes nonradiative decay to generate localized heat gradients, thereby enabling a complementary reactivity for

Received: January 12, 2024 Revised: March 12, 2024 Accepted: March 13, 2024 Published: March 20, 2024





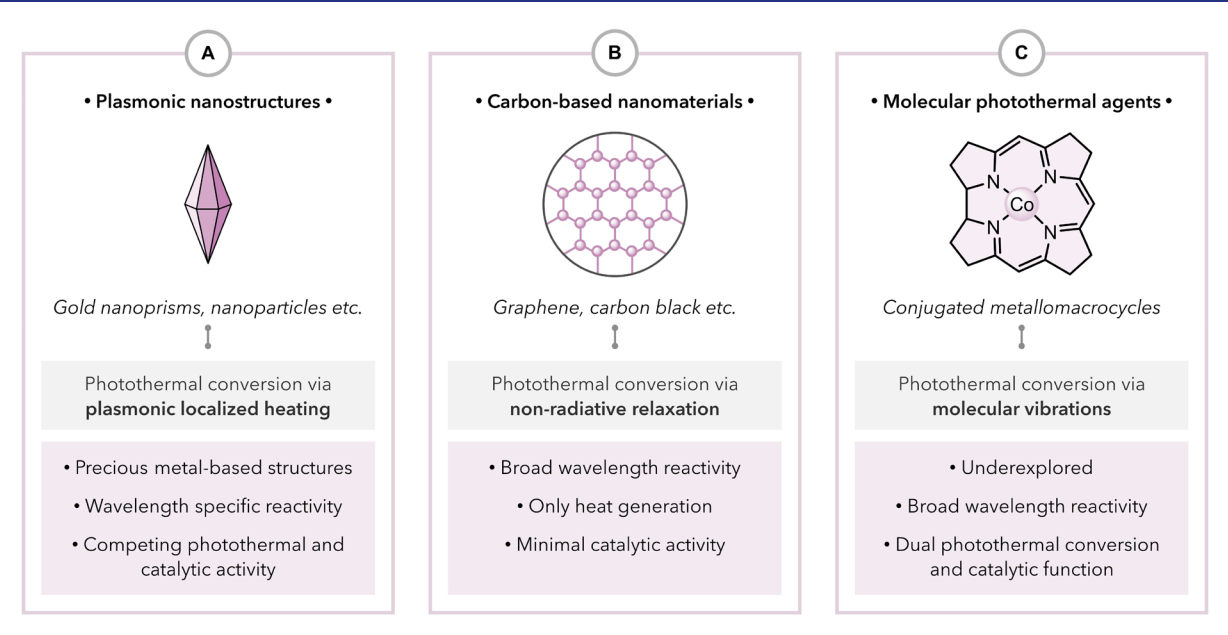


Figure 1. Mechanisms of photothermal conversion pathways via (A) plasmonic nanostructures, (B) carbon-based nanomaterials, and (C) molecular photothermal agents.

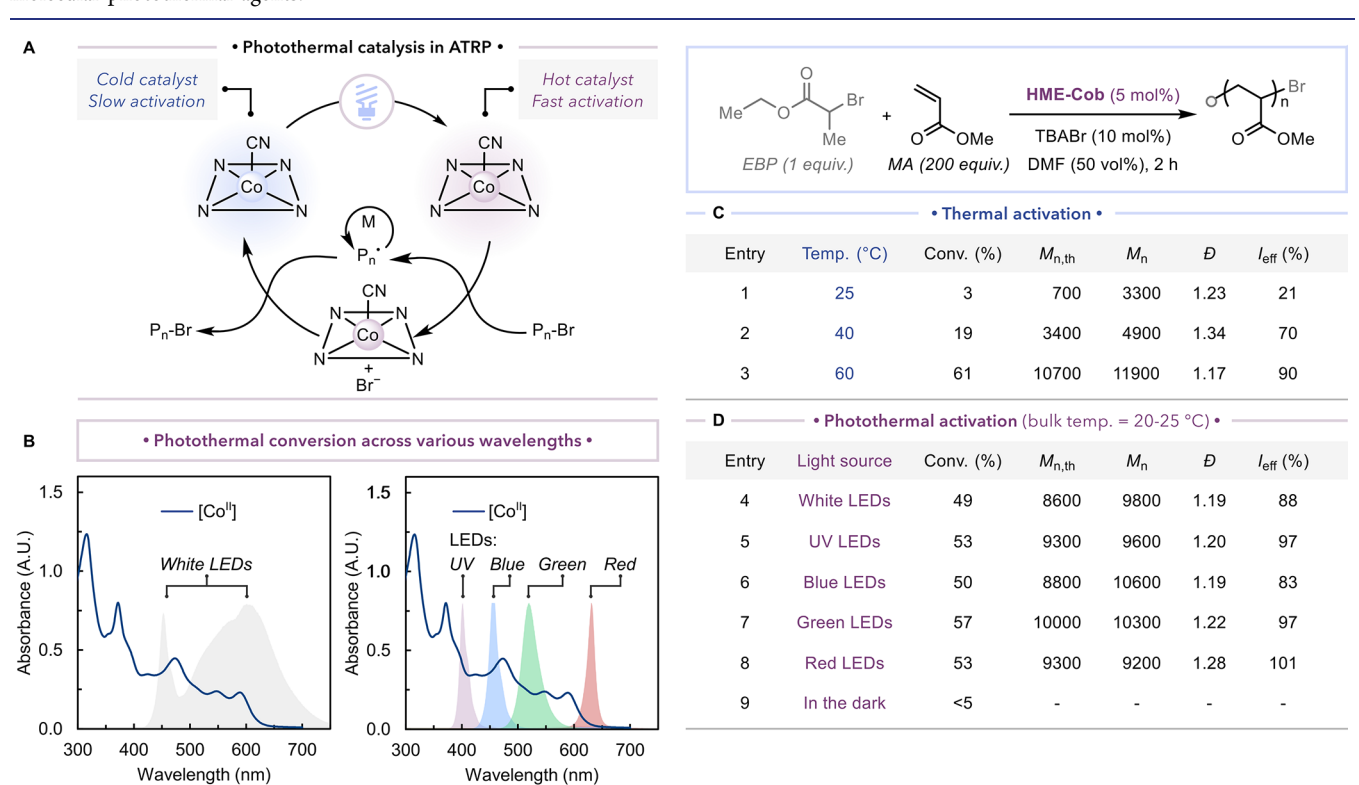


Figure 2. (A) Reaction scheme. (B) Absorption spectra of HME-Cob after reduction and emission spectra of all light sources used. (C) Polymerization via bulk heating in oil bath. (D) Polymerization via photothermal conversion with different wavelengths. Conditions: [MA]/[EBP]/[HME-Cob]/[TBABr] = 200/1/0.05/0.10 in DMF (50 vol %); the catalyst prereduced via $[HME-Cob]/[Zn]/[NH_4Cl] = 1/0.5/1$. Relative intensity output for all light sources was kept at 0.08 W.

thermal catalysis of the ATRP process. This strategy would promote thermal polymerization with temporal control under visible light (Figure 2A).

Polymerization of methyl acrylate (MA) with prereduced HME-Cob in the presence of ethyl 2-bromoproprionate (EBP) provided high monomer conversion with controlled molecular weight in bulk heating (temperatures = ~ 60 °C) (Figure 2C). The activity and polymerization efficiency of the catalyst

diminished at decreased temperatures, which resulted in <20% monomer conversions below 40 °C (Figure S2). Irradiation of a polymerization solution containing HME-Cob (5 mol % with respect to the EBP initiator) under white LEDs enabled photothermal conversion catalysis, thereby providing ~50% monomer conversion in 2 h with control over the molecular weight and dispersity (Figure 2D, entry 4). We hypothesized that this complex would be activated to convert light to heat

across a broad spectrum of light because HME-Cob has an absorption profile ranging from 300–600 nm ($\varepsilon=\sim$ 4000–9000 M $^{-1}$ cm $^{-1}$) (Figure 2B). Gratifyingly, we observed similar monomer conversions using LED lights in various wavelengths under the same intensity output (Figures 2D, S5, and S6). These results indicate wavelength-independent behavior of HME-Cob as a photothermal catalyst. In contrast, the polymerization efficiency of photoredox catalysts often depends on their absorption profile and the incident light. $^{27-29}$

To determine the photophysics of the HME-Cob, ultrafast laser spectroscopy was used to elucidate the reactivity when photoexcited. Upon photon absorption, HME-Cob(III) exhibited exponential decay with time scales of 30 and 200 ps (Figure S8). Upon reduction the complex (CoII) showed a change in dynamics with triexponential decay with time scales of 0.5, 4.6, and 80 ps (Figure S9). The 0.5 ps component is attributed to metal-to-ligand charge transfer with a back electron transfer that occurred on a 4.6 ps time scale where the 80 ps components are spectrally identical to unreduced HME-Cob. Addition of the EBP initiator changed the excited-state dynamics of HME-Cob, which indicated coordination of the alkyl halide to the complex. A triexponential decay with modified dynamics was observed and attributed to a charge transfer complex with the ligand. A forward electron transfer with 0.5 ps, followed by back electron transfer, occurred on a slower time scale of 34 ps (Figure S10). A longer lifetime of 280 ps was also observed with small features, which indicates that almost all photon absorption leads to rapid decay to the ground state with low quantum yields when photoexcited. Because of the formation of similar spectral features in the absence of the initiator, energy transfer can be ruled out.

To further probe the photothermal behavior of the catalyst, a thermal imaging camera monitored the effect of photothermal conversion on the bulk temperature of the reaction (Figure 3 and Figure S11). Rapid temperature increase

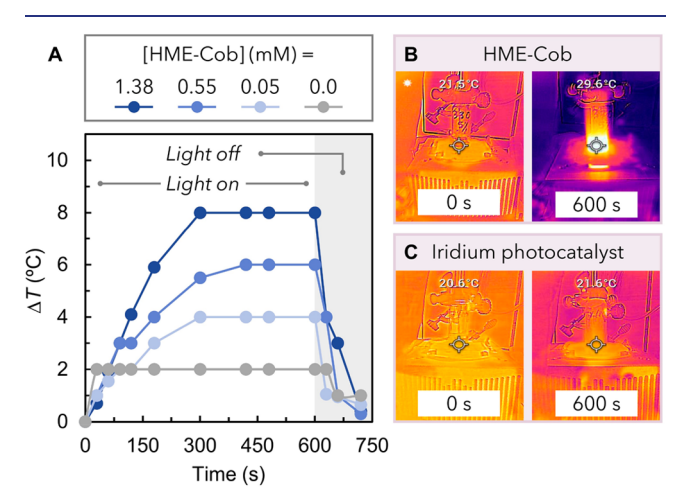


Figure 3. Changes in bulk reaction temperature using HME-Cob (A and B) compared with an iridium-based photoredox catalyst (C) under a white LED chip (relative intensity output 1.89 W).

occurred in a solution of HME-Cob (1.38 μ M in DMF) and reached a change in bulk temperature of 8 °C after 2 min. At reduced catalyst concentrations (0.55 and 0.05 μ M, respectively), the bulk temperature increase was lower and slightly slower than observed with a higher catalyst loading. These observations have been noted in other photothermal porphyrin reactions where intense heat is generated soon after

light exposure until reaching a constant bulk temperature. ^{1,21,30} In the absence of the catalyst, the temperature increased by 2 °C after 10 min of light exposure, thereby showing that HME-Cob generates additional heat. In comparison, a traditional iridium-based photoredox catalyst showed no bulk temperature increase, which further highlights the reactivity of the cobyrinate complex enabling photothermal conversion catalysis (Figure 3C and Figure S12). These temperature changes reflect only the bulk temperature of the solution, whereas the thermal gradients generated by the catalyst are much higher in its proximity, which leads to increased photothermal catalytic efficiency for polymerization reactions. Once the light was turned off, the temperature decreased sharply.

Polymerization kinetics using 5 mol % HME-Cob was monitored under white LED irradiation (Figure 4). Control over the polymerization was achieved with molecular weights in agreement with theoretical values and low dispersity (D <1.2). However, the polymerization rate decreased around 45 min, with the monomer conversion stalling at ~60% (Figure 4B). Using 2 mol % of the catalyst, polymerization of MA reached 29% monomer conversion (Figure S13), which indicates the effect of irreversible termination reactions that convert the activator catalyst to the deactivator species, $\lceil \text{Co}^{\text{III}} \rceil / \text{Br.}^{26,31}$ To circumvent this plateau in kinetics, we used a visible-light-active photoinitiator, bisacylphosphine oxide (BAPO), to generate radicals for catalyst regeneration (Figure 4A). 32,33 Using 2 equiv of BAPO (10 mol %) with respect to HME-Cob (5 mol %), a substantial increase in the rate of polymerization was observed with near quantitative monomer conversions and agreement between theoretical and experimental molecular weights (Figures 4B and S16). Even faster polymerization rates and control can still be seen by using higher-intensity light (Figures S17 and S18). Notably, the addition of BAPO with 0.2 mol % catalyst loadings achieved high monomer conversion, albeit with lower efficiency and higher dispersity (Figure S19). Increasing the concentration of bromide anion in the polymerization to favor deactivation decreased the dispersity and resulted in better initiator efficiency when using 0.5 and 0.2 mol % of HME-Cob (Figure 4I).

Structural analysis of the resulting polymers obtained at low catalyst loadings by ¹H NMR spectroscopy confirmed the presence of bromine chain-end functionality where all the polymer chains were initiated by the EBP initiator at catalyst concentrations as low as 0.2 mol % (Figures S27 and S28 for chain extension experiments).

Using photothermal conversion catalysis, we hypothesized that irradiation would subject the polymerization to temporal control. After four trials of on/off intervals, the reaction reached a conversion of ~70% with excellent temporal control (Figure 4E). We were pleased to observe that polymerization was reactivated even after a longer off period where the reaction was left in the dark for 30 min and reactivated for 5 min to give 53% monomer conversion, identical to what is seen during continuous irradiation (Figure 4F and Figure S20). Conversely, temporal control is not adequately achieved under bulk heating conditions because polymerization continues after removal of the heat source (Figures S23, S29, and S30). This observation showcases how photothermally generated thermal gradients provide excellent temporal control. This temporal control is a feature that cannot be achieved on demand with commonly used copper-based catalysts in ATRP.³⁴ While light irradiation enables catalyst regeneration to activate polymer-

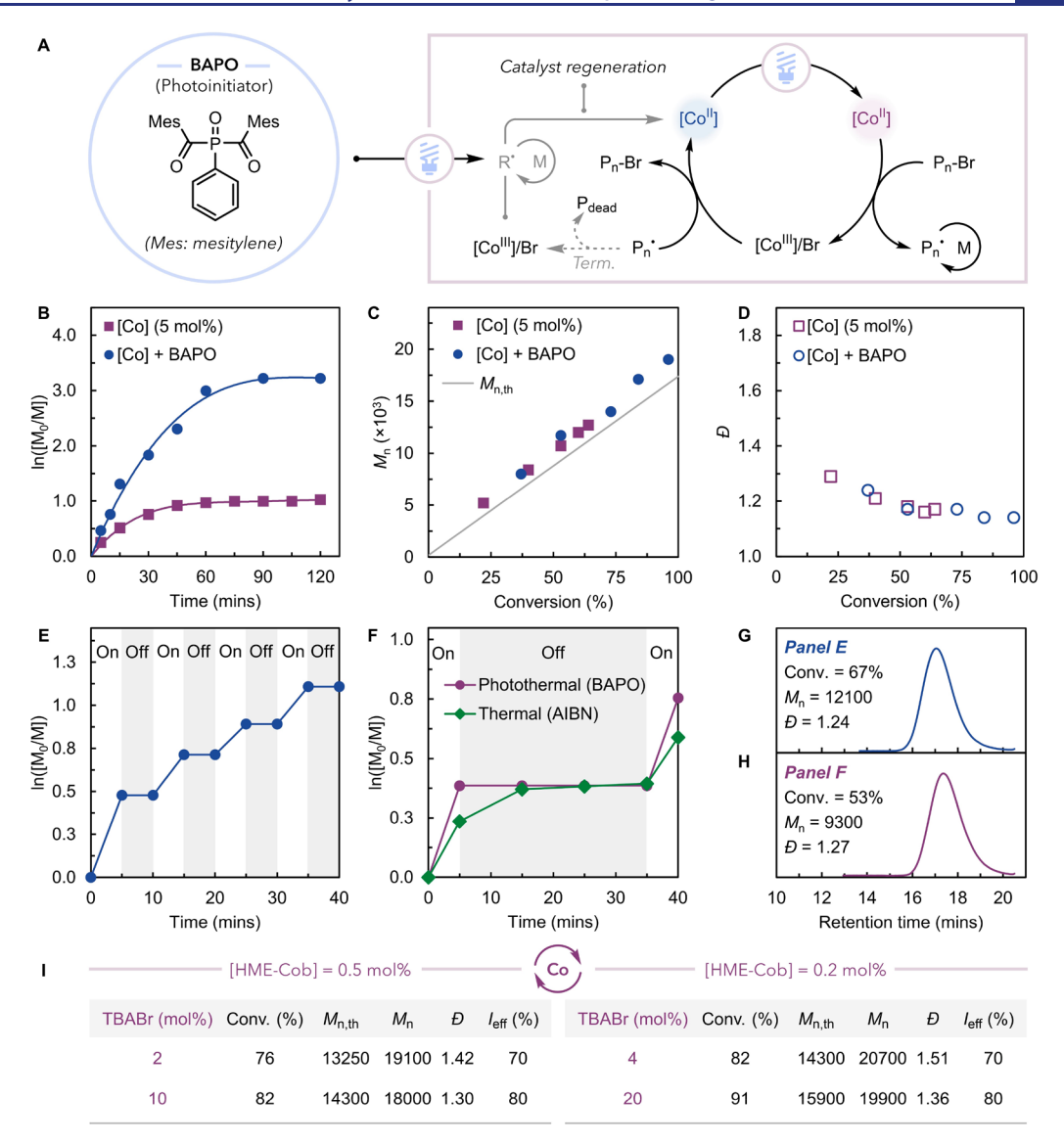


Figure 4. Kinetics of the polymerization of MA using HME-Cob as a photothermal catalyst. (A) Schematic representation of the ATRP catalytic cycle where exogenous radicals via photolysis of BAPO allow for catalyst regeneration. (B) Kinetics of the polymerization, (C) evolution of molecular weight (M_n) , and (D) dispersity (D) of resulting polymers using HME-Cob (5 mol %) in the presence or absence of BAPO photoinitiator. (E,F) Temporal control of polymerization via intermittent light on/off periods. Thermal polymerization was conducted at 60 °C in the dark using azobis(isobutyronitrile) (AIBN, 0.2 equiv) by placing the vial in/out of oil bath for temporal control. (G,H) GPC analysis of resulting polymers. Conditions: [MA]/[EBP]/[HME-Cob]/[TBABr]/[BAPO] = 200/1/0.05/0.10/0.10 in DMF under white LEDs (relative intensity output of 0.2 W). (I) Polymerizations at low catalyst concentrations.

ization with copper complexes, switching the light off does not immediately stop the reaction.³⁵ In contrast, we directly controlled the activity of the cobalt catalyst and achieved excellent temporal behavior in polymerization via photothermal conversion.

Lastly, given our ability to photocontrol the polymerization with visible light, we envisioned that this photothermal conversion catalyst could also be controlled with near-infrared (NIR) irradiation. Previous work achieved in NIR polymerization required special photosensitizers as copper complexes show no photocatalytic reactivity under NIR light and require long irradiation times for modest conversion. Despite the low absorptivity of the HME-Cob complex in the NIR region, photothermal conversion catalysis without additional photosensitizers activated polymerization (Figure 5A). Under these conditions, monomer conversion reached ~40% after 2 h

(Figure 5B). Reasonable control over the polymerization was achieved with dispersity around 1.30 and initiator efficiencies ~80% (Figure 5C). Gratifyingly, excellent temporal control was maintained with polymerization ceasing during off periods (Figures 5D,E), thereby signifying the versatility of this photocontrolled process across a broad range of wavelengths. Higher monomer conversion can be obtained by the addition of BAPO to the reaction for subsequent catalyst regeneration under white LEDs to confirm the polymerization control under NIR (Figure S24).

Here, we have demonstrated a vitamin B_{12} derivative as a molecular photothermal catalyst that efficiently converts visible light to thermal energy. Localized heat gradients generated via photothermal conversion by the cobyrinate complex increase its catalytic reactivity to allow photocontrolled cobalt-catalyzed ATRP. The efficiency of cobyrinate as a photothermal catalyst

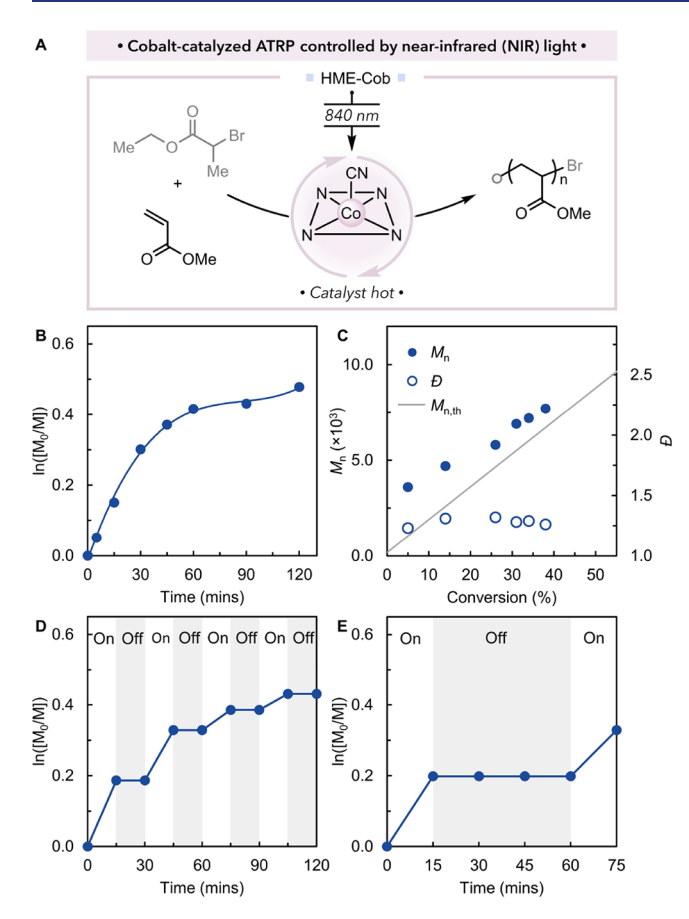


Figure 5. (A) Polymerization scheme of MA using HME-Cob as a photothermal catalyst under near-infrared light. (B) Kinetics of the polymerization. (C) Evolution of molecular weight (M_n) and dispersity (D) as a function of monomer conversion. (D,F) Temporal control via intermittent light on/off periods. Conditions: [MA]/[EBP]/[HME-Cob]/[TBABr]/[BAPO] = 200/1/0.05/0.10/0.10 in DMF. Relative intensity output, 1.0 W.

was demonstrated in catalyzing ATRP reactions in a controlled manner under visible or NIR light irradiation, thereby enabling excellent temporal control over polymerization.

ASSOCIATED CONTENT

Supporting Information

The Supporting Information is available free of charge at https://pubs.acs.org/doi/10.1021/jacs.4c00562.

Details of experimental procedure, additional polymerization experiments exploring the effect of catalyst concentration, alkyl halide initiators, and chain extension experiments with the GPC and NMR analysis of polymers (PDF)

AUTHOR INFORMATION

Corresponding Author

Erin E. Stache — Department of Chemistry, Princeton University, Princeton, New Jersey 08544, United States; orcid.org/0000-0002-4670-9117; Email: estache@princeton.edu

Authors

Cristina Preston-Herrera — Department of Chemistry, Princeton University, Princeton, New Jersey 08544, United States

- Sajjad Dadashi-Silab Department of Chemistry, Princeton University, Princeton, New Jersey 08544, United States;
 orcid.org/0000-0002-4285-5846
- Daniel G. Oblinsky Department of Chemistry, Princeton University, Princeton, New Jersey 08544, United States; orcid.org/0000-0001-7460-8260
- Gregory D. Scholes Department of Chemistry, Princeton University, Princeton, New Jersey 08544, United States; orcid.org/0000-0003-3336-7960

Complete contact information is available at: https://pubs.acs.org/10.1021/jacs.4c00562

Notes

The authors declare no competing financial interest.

ACKNOWLEDGMENTS

Financial support was provided in part by Princeton University, the National Science Foundation award CHE-1531632 for polymerization optimization and kinetic studies, and the National Institutes of Health award R35GM150839 for photothermal conversion studies. This work made use of the NMR and Ultrafast Laser Spectroscopy Facilities at Princeton University.

REFERENCES

- (1) Song, C.; Wang, Z.; Yin, Z.; Xiao, D.; Ma, D. Principles and Applications of Photothermal Catalysis. *Chem. Catal.* **2022**, 2 (1), 52–83.
- (2) Xu, C.; Ye, R.; Shen, H.; Lam, J. W. Y.; Zhao, Z.; Zhong Tang, B. Molecular Motion and Nonradiative Decay: Towards Efficient Photothermal and Photoacoustic Systems. *Angew. Chem., Int. Ed.* **2022**, *61* (30), No. e202204604.
- (3) Jauffred, L.; Samadi, A.; Klingberg, H.; Bendix, P. M.; Oddershede, L. B. Plasmonic Heating of Nanostructures. *Chem. Rev.* **2019**, *119* (13), 8087–8130.
- (4) Cui, X.; Ruan, Q.; Zhuo, X.; Xia, X.; Hu, J.; Fu, R.; Li, Y.; Wang, J.; Xu, H. Photothermal Nanomaterials: A Powerful Light-to-Heat Converter. *Chem. Rev.* **2023**, *123* (11), 6891–6952.
- (5) Zhao, L.; Liu, Y.; Xing, R.; Yan, X. Supramolecular Photothermal Effects: A Promising Mechanism for Efficient Thermal Conversion. *Angew. Chem., Int. Ed.* **2020**, *59* (10), 3793–3801.
- (6) Johnson, R. J. G.; Haas, K. M.; Lear, B. J. Fe3O4 Nanoparticles as Robust Photothermal Agents for Driving High Barrier Reactions under Ambient Conditions. *Chem. Commun.* **2015**, *51* (2), 417–420.
- (7) Haas, K. M.; Lear, B. J. Billion-Fold Rate Enhancement of Urethane Polymerization via the Photothermal Effect of Plasmonic Gold Nanoparticles. *Chem. Sci.* **2015**, *6* (11), 6462–6467.
- (8) Lemcoff, N.; Nechmad, N. B.; Eivgi, O.; Yehezkel, E.; Shelonchik, O.; Phatake, R. S.; Yesodi, D.; Vaisman, A.; Biswas, A.; Lemcoff, N. G.; Weizmann, Y. Plasmonic Visible—near Infrared Photothermal Activation of Olefin Metathesis Enabling Photoresponsive Materials. *Nat. Chem.* 2023, 15 (4), 475–482.
- (9) Han, B.; Zhang, Y.-L.; Chen, Q.-D.; Sun, H.-B. Carbon-Based Photothermal Actuators. *Adv. Funct. Mater.* **2018**, 28 (40), No. 1802235.
- (10) Steinhardt, R. C.; Steeves, T. M.; Wallace, B. M.; Moser, B.; Fishman, D. A.; Esser-Kahn, A. P. Photothermal Nanoparticle Initiation Enables Radical Polymerization and Yields Unique, Uniform Microfibers with Broad Spectrum Light. *ACS Appl. Mater. Interfaces* **2017**, *9* (44), 39034–39039.
- (11) Loeb, S.; Li, C.; Kim, J.-H. Solar Photothermal Disinfection Using Broadband-Light Absorbing Gold Nanoparticles and Carbon Black. *Environ. Sci. Technol.* **2018**, *52* (1), 205–213.
- (12) Dean, L. M.; Ravindra, A.; Guo, A. X.; Yourdkhani, M.; Sottos, N. R. Photothermal Initiation of Frontal Polymerization Using

- Carbon Nanoparticles. ACS Appl. Polym. Mater. 2020, 2 (11), 4690–4696.
- (13) Phillips, S. J.; Ginder, N. C.; Lear, B. J. Rapid Photothermal Synthesis of Polyurethane from Blocked Isocyanates. *Macromolecules* **2022**, *55* (16), 7232–7239.
- (14) Kugelmass, L. H.; Tagnon, C.; Stache, E. E. Photothermal Mediated Chemical Recycling to Monomers via Carbon Quantum Dots. J. Am. Chem. Soc. 2023, 145 (29), 16090–16097.
- (15) Matter, M. E.; Čamdžić, L.; Stache, E. E. Photothermal Conversion by Carbon Black Facilitates Aryl Migration by Photon-Promoted Temperature Gradients. *Angew. Chem., Int. Ed.* **2023**, *62* (40), No. e202308648.
- (16) Launay, V.; Caron, A.; Noirbent, G.; Gigmes, D.; Dumur, F.; Lalevée, J. NIR Organic Dyes as Innovative Tools for Reprocessing/Recycling of Plastics: Benefits of the Photothermal Activation in the Near-Infrared Range. *Adv. Funct. Mater.* **2021**, *31* (7), No. 2006324.
- (17) Müller, P.; Li, X.-P.; Niyogi, K. K. Non-Photochemical Quenching. A Response to Excess Light Energy. *Plant Physiol.* **2001**, *125* (4), 1558–1566.
- (18) Bricker, W. P.; Shenai, P. M.; Ghosh, A.; Liu, Z.; Enriquez, M. G. M.; Lambrev, P. H.; Tan, H.-S.; Lo, C. S.; Tretiak, S.; Fernandez-Alberti, S.; Zhao, Y. Non-Radiative Relaxation of Photoexcited Chlorophylls: Theoretical and Experimental Study. *Sci. Rep.* **2015**, *S* (1), No. 13625.
- (19) Zhao, Y.; Lin, J.; Kundrat, D. M.; Bonmarin, M.; Krupczak, J., Jr.; Thomas, S. V.; Lyu, M.; Shi, D. Photonically-Activated Molecular Excitations for Thermal Energy Conversion in Porphyrinic Compounds. J. Phys. Chem. C 2020, 124 (2), 1575–1584.
- (20) Jung, H. S.; Verwilst, P.; Sharma, A.; Shin, J.; Sessler, J. L.; Kim, J. S. Organic Molecule-Based Photothermal Agents: An Expanding Photothermal Therapy Universe. *Chem. Soc. Rev.* **2018**, 47 (7), 2280–2297.
- (21) Zhuo, C.; Cao, H.; You, H.; Liu, S.; Wang, X.; Wang, F. Two-in-One: Photothermal Ring-Opening Copolymerization of CO2 and Epoxides. ACS Macro Lett. 2022, 11 (7), 941–947.
- (22) Wdowik, T.; Gryko, D. C–C Bond Forming Reactions Enabled by Vitamin B₁₂—Opportunities and Challenges. *ACS Catal.* **2022**, *12* (11), 6517–6531.
- (23) Giedyk, M.; Gryko, D. Vitamin B12: An Efficient Cobalt Catalyst for Sustainable Generation of Radical Species. *Chem. Catal.* **2022**, 2 (7), 1534–1548.
- (24) Rury, A. S.; Wiley, T. E.; Sension, R. J. Energy Cascades, Excited State Dynamics, and Photochemistry in Cob(III)Alamins and Ferric Porphyrins. *Acc. Chem. Res.* **2015**, *48* (3), 860–867.
- (25) Shiang, J. J.; Cole, A. G.; Sension, R. J.; Hang, K.; Weng, Y.; Trommel, J. S.; Marzilli, L. G.; Lian, T. Ultrafast Excited-State Dynamics in Vitamin B ₁₂ and Related Cob(III)Alamins. *J. Am. Chem. Soc.* **2006**, *128* (3), 801–808.
- (26) Dadashi-Silab, S.; Preston-Herrera, C.; Stache, E. E. Vitamin B Derivative Enables Cobalt-Catalyzed Atom Transfer Radical Polymerization. *J. Am. Chem. Soc.* **2023**, *145* (35), 19387–19395.
- (27) Treat, N. J.; Sprafke, H.; Kramer, J. W.; Clark, P. G.; Barton, B. E.; Read de Alaniz, J.; Fors, B. P.; Hawker, C. J. Metal-Free Atom Transfer Radical Polymerization. *J. Am. Chem. Soc.* **2014**, *136* (45), 16096–16101.
- (28) Corbin, D. A.; Miyake, G. M. Photoinduced Organocatalyzed Atom Transfer Radical Polymerization (O-ATRP): Precision Polymer Synthesis Using Organic Photoredox Catalysis. *Chem. Rev.* **2022**, 122 (2), 1830–1874.
- (29) Hu, X.; Szczepaniak, G.; Lewandowska-Andralojc, A.; Jeong, J.; Li, B.; Murata, H.; Yin, R.; Jazani, A. M.; Das, S. R.; Matyjaszewski, K. Red-Light-Driven Atom Transfer Radical Polymerization for High-Throughput Polymer Synthesis in Open Air. *J. Am. Chem. Soc.* **2023**, 145 (44), 24315–24327.
- (30) Lyu, M.; Lin, J.; Krupczak, J.; Shi, D. Solar Harvesting through Multilayer Spectral Selective Iron Oxide and Porphyrin Transparent Thin Films for Photothermal Energy Generation. *Adv. Sustain. Syst.* **2021**, *5* (6), No. 2100006.

- (31) Jakubowski, W.; Min, K.; Matyjaszewski, K. Activators Regenerated by Electron Transfer for Atom Transfer Radical Polymerization of Styrene. *Macromolecules* **2006**, 39 (1), 39–45.
- (32) Müller, S. M.; Schlögl, S.; Wiesner, T.; Haas, M.; Griesser, T. Recent Advances in Type I Photoinitiators for Visible Light Induced Photopolymerization. *ChemPhotoChem.* **2022**, 6 (11), No. e202200091.
- (33) Kolczak, U.; Rist, G.; Dietliker, K.; Wirz, J. Reaction Mechanism of Monoacyl- and Bisacylphosphine Oxide Photoinitiators Studied by 31P-, 13C-, and 1H-CIDNP and ESR. *J. Am. Chem. Soc.* **1996**, *118* (27), 6477–6489.
- (34) Dadashi-Silab, S.; Lee, I.-H.; Anastasaki, A.; Lorandi, F.; Narupai, B.; Dolinski, N. D.; Allegrezza, M. L.; Fantin, M.; Konkolewicz, D.; Hawker, C. J.; Matyjaszewski, K. Investigating Temporal Control in Photoinduced Atom Transfer Radical Polymerization. *Macromolecules* **2020**, *53* (13), 5280–5288.
- (35) Lorandi, F.; Fantin, M.; Matyjaszewski, K. Atom Transfer Radical Polymerization: A Mechanistic Perspective. *J. Am. Chem. Soc.* **2022**, *144* (34), 15413–15430.
- (36) Kütahya, C.; Schmitz, C.; Strehmel, V.; Yagci, Y.; Strehmel, B. Near-Infrared Sensitized Photoinduced Atom-Transfer Radical Polymerization (ATRP) with a Copper(II) Catalyst Concentration in the Ppm Range. *Angew. Chem., Int. Ed.* **2018**, *57* (26), 7898–7902.